

ChemComm

Accepted Manuscript



This is an *Accepted Manuscript*, which has been through the Royal Society of Chemistry peer review process and has been accepted for publication.

Accepted Manuscripts are published online shortly after acceptance, before technical editing, formatting and proof reading. Using this free service, authors can make their results available to the community, in citable form, before we publish the edited article. We will replace this *Accepted Manuscript* with the edited and formatted *Advance Article* as soon as it is available.

You can find more information about *Accepted Manuscripts* in the [Information for Authors](#).

Please note that technical editing may introduce minor changes to the text and/or graphics, which may alter content. The journal's standard [Terms & Conditions](#) and the [Ethical guidelines](#) still apply. In no event shall the Royal Society of Chemistry be held responsible for any errors or omissions in this *Accepted Manuscript* or any consequences arising from the use of any information it contains.

of the core, a silica based hollow sphere is derived (Fig. S1b). The exterior surface of the shell should be terminated with the imidazolin group, while the interior surface is the phenyl group. Imidazolin based Janus nanosheets are achieved after crushing the parent Janus hollow sphere by colloid milling. Two sides of the Janus nanosheets are smooth (Fig. 1b). A representative Janus nanosheet about 65 ± 2 nm thick is used as the example (Fig. S2). In order to confirm distinct compartmentalization of the imidazolin group exclusively onto one side, negatively charged trisodium citrate capped Fe_3O_4 nanoparticles are used to label the imidazolin side by a specific interaction. As a result, the imidazolin side becomes coarsening, while the other side remains smooth (Fig. 1c). The nanosheets are well dispersible both in oil and water (Fig. 1d), revealing Janus performance.

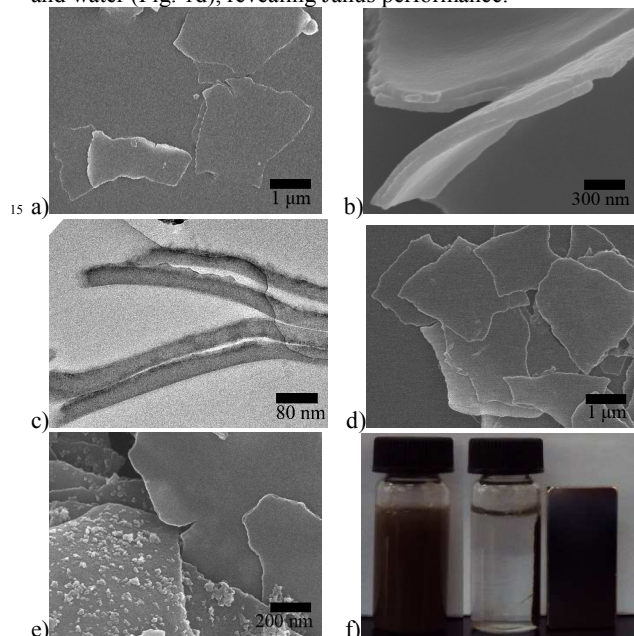


Figure 2. The representative IL-Janus silica nanosheets. a) SEM image of the Cl^- based IL-Janus nanosheet powder after naturally drying the aqueous dispersion; b) SEM image of the Cl^- based IL-Janus nanosheet powder after cryo-drying the aqueous dispersion; c) cross-section TEM image of the nanosheet powder embedded in PMMA; d) SEM images of the Cl^- based IL-Janus nanosheets which are dried from the ethanol; e) SEM image of the IL-Janus Fe_3O_4 composite nanosheets, and f) the dispersion in water (left) and

collected with a magnet (right). After a selective reaction with alkyl halide such as 1-chlorobutane, the imidazolin side becomes ionic liquid functionalized, while the other phenyl- side preserves the hydrophobic. The white powder becomes yellow after this ionic liquid functionalization. Both sides remain smooth. Zeta potential of the IL based Janus nanosheets is $+38.1$ mV at $\text{pH}=7.0$ (Fig. S3). In comparison, Zeta potential of the imidazolin based Janus nanosheets is $+17.2$ mV since pK_a (7.2–7.4) of imidazolin is slightly above 7.0. Reaction extent is determined by surface element analysis (Fig. S4). The N1s peak at 409.9 eV is assigned to imidazolin, which is about 3%. Cl element is 0.9 % after the ionic liquid functionalization. The IL based Janus nanosheets remain well dispersed both in water and oil due to their amphiphilic performance (Fig. S5). In selective solvents for example water, the Janus nanosheets should be back-to-back aggregated but dispersible with the hydrophilic sides exposed to the aqueous continuous phase. After naturally drying the aqueous dispersion, a kind of bi-layered superstructure is observed (Fig.

2a). In order to freeze the aggregation structure in the dispersion, cryo-drying of the dilute dispersion is employed. As shown in Figure 2b, the Janus nanosheets form the 1:1 back-to-back aggregation bi-layered superstructure. The 1:1 aggregation is further convinced by cross-section TEM observation (Fig. 2c). As comparison, in co-solvents for example ethanol no aggregation is found but individual nanosheet (Fig. 2d). Trisodium citrate capped Fe_3O_4 nanoparticles can be absorbed exclusively onto the ionic liquid side (Fig. 2e), whilst the other side remains smooth. The Fe_3O_4 contained IL based Janus composite nanosheets preserve the Janus performance. They can be simply manipulated with a magnet (Fig. 2f).

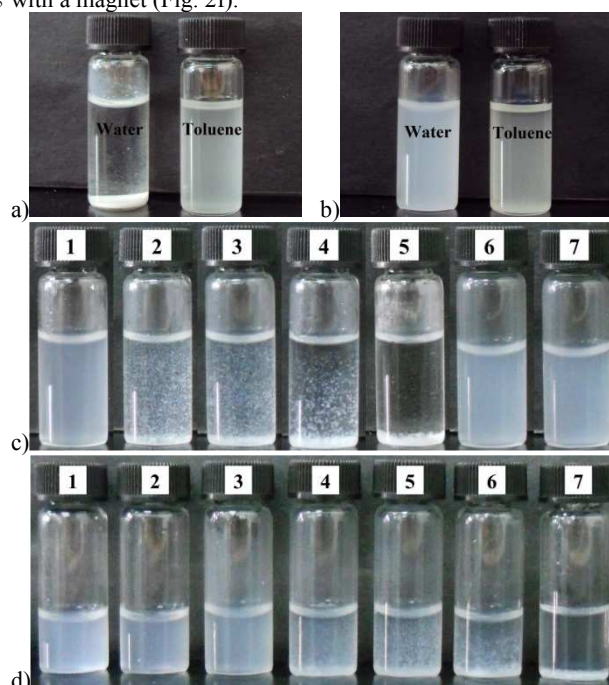


Figure 3. a) PF_6^- based IL-hydrophobic nanosheets which are aggregated in water (left) and dispersible in toluene (right); b) BF_4^- based IL-Janus nanosheets which are dispersible both in water (left) and in toluene (right); c) Janus-hydrophobic reversible transformation of the representative Cl^- based IL-Janus nanosheets. 6 μmol of KPF_6 is added into the aqueous dispersion after varied time (min): (1) 0, (2) 2, (3) 5, (4) 8, (5) 10; and 6 μmol of NaCl is added in the system (c5) after varied time: (6) 20 s, (7) 1 h; d) Janus-hydrophobic transformation of the Cl^- based IL-Janus nanosheets with varied feeding amount of KPF_6 (μmol): (1) 0, (2) 2, (3) 4, (4) 4.5, (5) 5, (6) 5.5, (7) 6. All the samples stand for 10 min.

Composition of the IL layer is tunable by simple exchanging anions, meanwhile wettability of the layer is reversibly switchable between hydrophilic and hydrophobic. As an example, after Cl^- is exchanged with PF_6^- , the nanosheets become only dispersible in toluene not in water (Fig. 3a). This reveals that the IL side becomes hydrophobic. After the PF_6^- group is exchanged with BF_4^- , the nanosheets again become dispersible both in oil and water (Fig. 3b). This indicates that Janus performance of the nanosheet has recovered. Morphology of the nanosheet is not influenced by the ion exchange (Fig. S6 a-b). The anion exchanging is general. Along the similar routine, $(\text{CF}_3\text{SO}_2)_2\text{N}^-$, HSO_4^- based IL-Janus nanosheets are derived (Fig. S6 c-f). Presence of the corresponding anionic groups is further confirmed by FT-IR (Fig. S7). The bands at $1650\text{--}1550\text{ cm}^{-1}$ are attributed to the imidazolium cation. The bands at $850\text{--}840\text{ cm}^{-1}$, $640\text{--}620\text{ cm}^{-1}$, $1360\text{--}1345\text{ cm}^{-1}$, and $1065\text{--}1055\text{ cm}^{-1}$ are attributed to the PF_6^- , HSO_4^- , $(\text{CF}_3\text{SO}_2)_2\text{N}^-$, and BF_4^- , respectively. The

anion exchange degree can be determined by surface XPS element analysis (Fig. S8). For example, presence of F and B elements is verified by XPS spectrum of the BF_4^- based IL-Janus nanosheets, whilst the Cl signal disappears completely. This indicates that the anion exchange has completely achieved.

The anion exchange process is fast (Fig. 3c). As an example, upon feeding $6 \mu\text{mol}$ of KPF_6 into the Cl^- based IL-Janus nanosheet aqueous dispersion, no Cl can be detected onto the nanosheets shortly after feeding KPF_6 within 20 s.^[30] The Janus nanosheets start to aggregate and progressively precipitate within minutes (Fig. 3c1-5). When $6 \mu\text{mol}$ of NaCl is fed into the above precipitation system under shaking, the nanosheets become redispersible in water within 20 s (Fig. 3c6). The dispersion keeps stable over hours (Fig. 3c7). This is consistent with the fast exchange of PF_6^- with Cl^- . Since anion exchange degree is tunable, wettability of the ionic liquid side thus dispersibility of the nanosheets can be controlled (Fig. 3d). As an example, after KPF_6 is fed into the Cl^- based IL-Janus nanosheet aqueous dispersion at varied amount, dispersibility is monitored to evaluate the wettability. At low level below $4 \mu\text{mol}$, the IL-Janus nanosheets remain well dispersible in water. This is understandable that a majority of Cl^- is preserved and hydrophilic performance of the IL side dominates. The XPS result reveals that Cl and PF_6^- fractions are comparable (Table S1). At an increased level of KPF_6 above $4.5 \mu\text{mol}$, PF_6^- dominates within the IL layer. The IL-Janus nanosheets precipitate from the aqueous dispersion. This indicates that the hydrophobic performance dominates. With the increase in KPF_6 feeding amount, the precipitation becomes faster. At high level of for example $6.0 \mu\text{mol}$, the nanosheets precipitate completely. SEM observation of the nanosheets in dispersion further confirms the aggregation with PF_6^- feeding amount (Fig. S9). The hydrophobic PF_6^- based IL-Janus nanosheets could be well dispersible in toluene. After drying, individual nanosheets are observed rather than aggregation (Fig. S10).

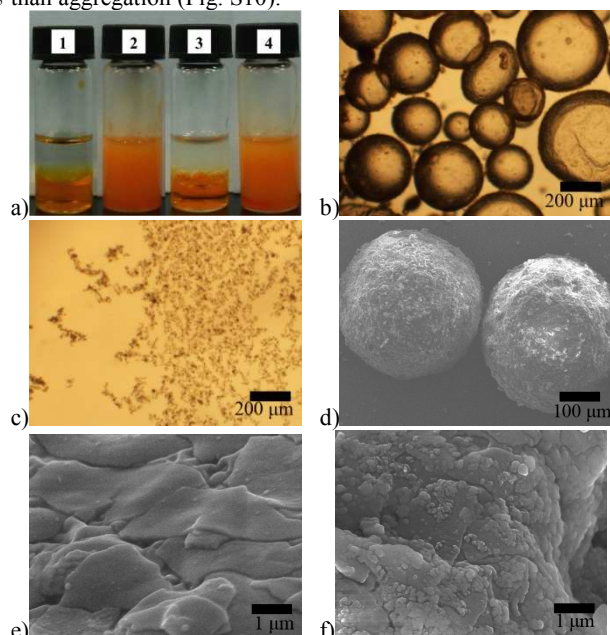


Figure 4. a) Janus performance of the IL-nanosheets as anion responsive surfactants: (1) an immiscible mixture of decane (top) and water (bottom), methyl orange is added to water as chromogenic agent; (2) oil-in-water emulsion stabilized with the Cl^- based IL-Janus nanosheets, decane/water

volume ratio is 3:2; (3) after feeding $10 \mu\text{mol}$ of KPF_6 in the emulsion (2), the emulsion destabilizes; (4) after feeding Cl^- again in the mixture (3), an emulsion forms; b) optical microscopy image of the decane-in-water emulsion (a2); c) optical microscopy image of the middle interface region in (a3); d) SEM image of the dispersed paraffin particles stabilized with the Cl^- based IL-Janus nanosheets, orientation of the Janus nanosheets is frozen at the interface after paraffin is cooled; e, f) magnified SEM images of the paraffin particle surface before and after being labelled with trisodium citrate capped Fe_3O_4 nanoparticles.

Let's demonstrate the representative Cl^- based IL-Janus nanosheets as a solid surfactant to emulsify immiscible liquids (Fig. 4a1) and anion triggered de-emulsification. As an example, an oil-in-water (o/w) emulsion forms at a decane/water volume ratio 3:2 (Fig. 4a2). The emulsion keeps stable over months. A trace amount of methyl orange is added into water phase for easy observation. The dispersed droplets are $100\text{-}500 \mu\text{m}$ in diameter (Fig. 4b), whose size decreases with the Janus nanosheet content. After drops of KPF_6 aqueous solution are added, the emulsion starts to de-emulsify within minutes. Water and oil separate into two immiscible layers eventually (Fig. 4a3). No droplets are observed but fragmental pieces (Fig. 4c). In comparison, in the case of imidazolin based Janus nanosheets, the emulsion keeps stable (Fig. S11a) even after KPF_6 is added. This means that only IL functionalized Janus nanosheets are ion responsive. If KCl is added instead of KPF_6 , the emulsion remains stable (Fig. S11b). This suggests that the IL-Janus nanosheets are responsive selectively to anions. After drops of NaCl aqueous solution are added, the immiscible liquids after phase separation become emulsified again in minutes, forming a stable emulsion (Fig. 4a4). It is noted that the anion triggered reversible transformation between emulsification and de-emulsification occurs without stirring if the continuous phase is aqueous. If oil phase is continuous, stirring is required to drive the transformation (Fig. S12). In order to observe orientation of the IL-Janus nanosheets at the interface, a melt-paraffin (T_m : $52\text{-}54 \text{ }^\circ\text{C}$) is emulsified in water using the Cl^- based IL-Janus nanosheets (Fig. 4d). After the emulsion is cooled down to room temperature, orientation of the IL-Janus nanosheets at the emulsion interface is frozen thereby (Fig. 4e). The nanosheets lay onto the interface. Trisodium citrate capped Fe_3O_4 nanoparticles are used to label the IL-Janus nanosheets. The coarsened side corresponding to the IL group terminated side faces the external aqueous phase (Fig. 4f).

In summary, we report a facile and universal method to synthesize ionic liquid functionalized Janus nanosheets. Wettability of the IL terminated side is triggered between hydrophilic and hydrophobic by anion exchanging. Accordingly, dispersibility of the nanosheets and stability of the emulsion with the IL-Janus nanosheets is triggered by anion exchanging in a reversible way. The transformation can be achieved regardless if the continuous phase is aqueous or oil. The idea can be extended to other IL-based Janus nanosheets with tunable cations.

This work was supported by the Basic Research Development Program (2012CB933200), the National Natural Science Foundation of China (51233007, 51173191, 51273087, 21071070), and the Foundation for Innovative Research Groups of Liaoning Provincial Universities (No. LT2011001).

Notes and references

¹⁰⁰ *a* State Key Laboratory of Polymer Physics and Chemistry, Institute of Chemistry, Chinese Academy of Sciences, Beijing 100190, China. Fax: 8610-62559373; Tel: 8610-82619206; E-mail: yangzz@iccas.ac.cn (Z.Y)

^b Liaoning Provincial Key Laboratory for Green Synthesis and Preparative Chemistry of Advanced Materials (Liaoning University), Shenyang 110036, China. Fax: 8624-62202380; Tel: 8624-62202378; E-mail: songlab@lnu.edu.cn (X. S)

[†] Electronic Supplementary Information (ESI) available: Experimental section and supplemental figures. See DOI: 10.1039/b000000x/

- 1 P. G. de Gennes, *Rev. Mod. Phys.* 1992, **64**, 645.
- 2 A. Walther and A. H. E. Müller, *Soft Matter* 2008, **4**, 663.
- 3 A. Perro, S. Reculosa, S. Ravaine, E. B. Bourgreat-Lami and E. Duguet, *J. Mater. Chem.* 2005, **15**, 3745.
- 4 S. C. Glötzer, *Science* 2004, **306**, 419.
- 5 D. Dendukuri, D. C. Pregibon, J. Collins, T.A. Hatton and P. S. Doyle, *Nat. Mater.* 2006, **5**, 365.
- 6 S. Jiang and S. Granick, Janus Particle Synthesis, Self-Assembly and Applications, RSC, Cambridge, 2012.
- 7 A. Walther, A. H. E. Müller, *Chem. Rev.* 2013, **113**, 5194.
- 8 F. X. Liang, J. G. Liu, C. L. Zhang, X. Z. Qu, J. L. Li and Z. Z. Yang, *Chem. Commun.* 2011, **47**, 1231.
- 9 A. Walther, X. André, M. Drechsler, V. Abetz and A. H. E. Müller, *J. Am. Chem. Soc.* 2007, **129**, 6187.
- 10 M. Lattuada and T. A. Hatton, *J. Am. Chem. Soc.* 2007, **129**, 12878.
- 11 T. Tanaka, M. Okayama, H. Minami and M. Okubo, *Langmuir* 2010, **26**, 11732.
- 12 H. Xie, Z. G. She, S. Wang, G. Sharma and J. W. Smith, *Langmuir* 2012, **28**, 4459.
- 13 A. Walther, K. Matussek, A. H. E. Müller, *ACS Nano* 2008, **2**, 1167.
- 14 Y. Nonomura, S. Komura, K. Tsujii, *Langmuir* 2004, **20**, 11821.
- 15 Y. Nonomura, S. Komura, K. Tsujii, *J. Phys. Chem. B* 2006, **110**, 13124.
- 16 J. R. Dorvee, A. M. Derfus, S. N. Bhatia and M. J. Sailor, *Nat. Mater.* 2004, **3**, 896.
- 17 F. X. Liang, K. Shen, X. Z. Qu, C. L. Zhang, Q. Wang, J. L. Li, J. G. Liu and Z. Z. Yang, *Angew. Chem. Int. Ed.* 2011, **50**, 2379.
- 18 S. H. Hu and X. H. ao, *J. Am. Chem. Soc.* 2010, **132**, 7234.
- 19 H. L. Yang, F. X. Liang, X. Wang, Y. Chen, C. L. Zhang, Q. Wang, X. Z. Qu, J. L. Li, D. C. Wu and Z. Z. Yang, *Macromolecules* 2013, **46**, 2754.
- 20 Y. Chen, F. X. Liang, H. L. Yang, C. L. Zhang, Q. Wang, X. Z. Qu, J. L. Li, Y. L. Cai, D. Qiu and Z. Z. Yang, *Macromolecules* **2012**, **45**, 1460.
- 21 B. S. Lee, Y. S. Chi, J. K. Lee, I. S. Choi, C. E. Song, S. K. Namgoong and S. Lee, *J. Am. Chem. Soc.* 2004, **126**, 480.
- 22 B. Yu, F. Zhou, G. Liu, Y. M. Liang, W. T. S. Huck and W. M. Liu, *Chem. Commun.* 2006, 2356.
- 23 X. Y. He, W. Yang and X. W. Pei, *Macromolecules* 2008, **41**, 4615.
- 24 J. Dupont, R. F. de Souza and P. A. Z. Suarez, *Chem. Rev.* 2002, **102**, 3667.
- 25 P. Wasserscheid and W. Keim, *Angew. Chem. Int. Ed.* 2000, **39**, 3772.
- 26 R. Sheldon, *Chem. Commun.* 2001, **23**, 2399.
- 27 A. C. Cole, J. L. Jensen, I. Ntai, K.L.T. Tran, K. J. Weave, D. C. Forbes and J. H. Davis, *J. Am. Chem. Soc.* 2002, **124**, 5962.
- 28 T. Welton, *Chem. Rev.* 1999, **99**, 2071.
- 29 L. A. Blanchard, D. Hancu, E. J. Beckman and J. F. Brennecke, *Nature* 1999, **399**, 28.
- 30 The samples for XPS measurement of the anion exchange degree were separated and purified by centrifugation after adding the salt. At a given centrifugation speed (6000 r / min), it took at least 20 s for the separation even upon adding the salt.